

## Spectroscopic Study of Colloidal $\text{VOPO}_4 \cdot 2\text{H}_2\text{O}$

C. R'KHA, M. T. VANDENBORRE, AND J. LIVAGE

*Laboratoire Spectrochimie du Solide, Université Pierre et Marie Curie, 4, place Jussieu, T. 44, 2ème étage, 75230 Paris Cedex 05, France*

AND R. PROST AND E. HUARD

*Station de Science du Sol—INRA—Route de Saint-Cyr, 78000 Versailles, France*

Received August 12, 1985; in revised form November 14, 1985

The sol-gel synthesis of  $\text{VOPO}_4 \cdot 2\text{H}_2\text{O}$  via a polycondensation process leads to colloidal particles that can be deposited onto a substrate to give layers. These layers exhibit a strong anisotropy arising from a stacking of the colloidal particles. More accurate information about the  $\text{VOPO}_4 \cdot 2\text{H}_2\text{O}$  structure can then be obtained by X-ray diffraction, ESR, and infrared experiments. They show that, in  $\text{VOPO}_4 \cdot 2\text{H}_2\text{O}$ , water molecules are bonded to vanadium ions along an axial position opposite to the  $\text{V}=\text{O}$  short bond. Another kind of water molecule appears in  $\text{VOPO}_4 \cdot 2\text{H}_2\text{O}$  where all water molecules seem to be linked together by hydrogen bonds making a double layer between the  $\text{VOPO}_4$  sheets. © 1986 Academic Press, Inc.

### Introduction

$\text{VOPO}_4$  exhibits a lamellar structure made of polymeric  $(\text{VOPO}_4)_n$  layers providing a host structure for the intercalation of guest species such as pyridine, primary amines, or alcohols (1). Water molecules can also be reversibly intercalated between these layers leading to hydrates such as  $\text{VOPO}_4 \cdot \text{H}_2\text{O}$  and  $\text{VOPO}_4 \cdot 2\text{H}_2\text{O}$  (2). This last one is a stable phase obtained under ambient conditions (3). Its complete dehydration leads to a vanadium mixed oxides such as  $\text{VOPO}_4$  (3) which is one of the oxidized phase of a catalytic redox active and selective in butene oxidation into malonic anhydride (4).

Many structural studies have been performed on the different  $\text{VOPO}_4 \cdot n\text{H}_2\text{O}$

phases (4-6), and several crystallographic structures have been found (7, 8). The one we are studying in this paper corresponds to  $\alpha\text{VOPO}_4 \cdot 2\text{H}_2\text{O}$ . It has a tetragonal structure with a space group  $P4/mmm$  and contains two formula units per unit cell. The  $(\text{VOPO}_4)_n$  layers are built up of  $(\text{VO}_5)$  chains linked together by  $(\text{PO}_4)$  tetrahedra (Fig. 1). Water molecules are intercalated between these layers. They lead to an increase of the  $c$  parameter from 4.11 Å for  $\text{VOPO}_4$  up to 6.30 Å for  $\text{VOPO}_4 \cdot \text{H}_2\text{O}$  and 7.41 Å for  $\text{VOPO}_4 \cdot 2\text{H}_2\text{O}$  (3).

$\text{VOPO}_4 \cdot 2\text{H}_2\text{O}$  single crystals are not large enough to allow X-ray diffraction studies so that structural information about the position of water molecules have only been obtained from neutron experiments performed on  $\text{VOPO}_4 \cdot 2\text{D}_2\text{O}$  powders (9).

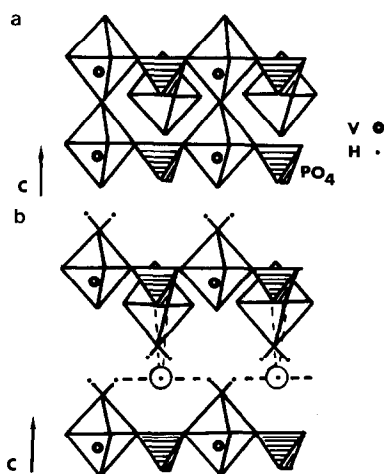


FIG. 1. Structure of VOPO<sub>4</sub> (a) and VOPO<sub>4</sub> · 2H<sub>2</sub>O (b) according to (3).

These show that one water molecule is directly bonded to a vanadium ion along an axial position opposite to the V=O short bond. The position of the other water molecule has not been determined accurately.

VOPO<sub>4</sub> · 2H<sub>2</sub>O is usually made by boiling H<sub>3</sub>PO<sub>4</sub> with V<sub>2</sub>O<sub>5</sub> during 16 hr (10). In this paper we suggest a new way for making VOPO<sub>4</sub> · 2H<sub>2</sub>O via the sol-gel process. This leads to colloidal particles that can easily be deposited onto a substrate to give oriented deposits that exhibit a strong dichroic character when studied by infrared absorption. This allows more accurate information about the position of water molecules.

### Synthesis of Colloidal VOPO<sub>4</sub> · 2H<sub>2</sub>O

Colloidal VOPO<sub>4</sub> · 2H<sub>2</sub>O was obtained according to a procedure already described for the synthesis of V<sub>2</sub>O<sub>5</sub> gels (11). An aqueous solution of sodium metavanadate (NaVO<sub>3</sub>, 0.5 mole/liter) is mixed to a slight excess of a sodium metaphosphate (NaPO<sub>3</sub>, 0.5 mole/liter) solution. This mixture is then passed through a proton exchange resin (Dowex 50 WX<sub>2</sub>, 50–100 mesh). A clear, pale yellow solution is obtained after ion

exchange. It spontaneously gives rise, after about half an hour, to shiny yellow precipitate of VOPO<sub>4</sub> · 2H<sub>2</sub>O. This precipitate is then washed with water to remove most of the phosphoric acid. It remains stable as long as the pH of the solution is kept below 4. A colloidal suspension is then obtained that can be easily deposited, like a paint, onto a glass substrate giving a thick layer that remains stable upon drying in air.

Oxovanadium phosphate VOPO<sub>4</sub> · 2H<sub>2</sub>O is slightly reduced when washed with acetone. It remains shiny, but turns to pale green suggesting an increase of the V(IV)/V(V) ratio (3).

All spectroscopic studies reported in this paper have been performed on VOPO<sub>4</sub> · 2H<sub>2</sub>O layers obtained by deposition. A strong anisotropy of the colloidal particles will then be evidenced.

### Structural Study of Colloidal VOPO<sub>4</sub> · 2H<sub>2</sub>O

The X-ray diffraction pattern on the yellow precipitate, performed on a ground powder and recorded on a powder 17-cm vertical X-ray diffractometer Philips PW 1050/25, is typical of VOPO<sub>4</sub> · 2H<sub>2</sub>O (4). The unit cell is tetragonal with the following parameters:  $a = b = 6.20 \text{ \AA}$ ,  $c = 7.41 \text{ \AA}$ .

The diffraction spectrum, recorded for a deposit on a platinum grid, and using a reflection geometry, however, appears completely different. It only exhibits a series of 00*l* peaks, the intensity of which continuously decreases down to the fifth order (Fig. 2a). Such a diagram is typical of a one dimensional order along a direction perpendicular to the substrate. It corresponds to a basal spacing  $d = 7.41 \text{ \AA}$ , showing that the stacking of the colloidal particles occurs along their *c* axis. The sharpness of Bragg's 00*l* peaks suggests that this stacking is very well ordered.

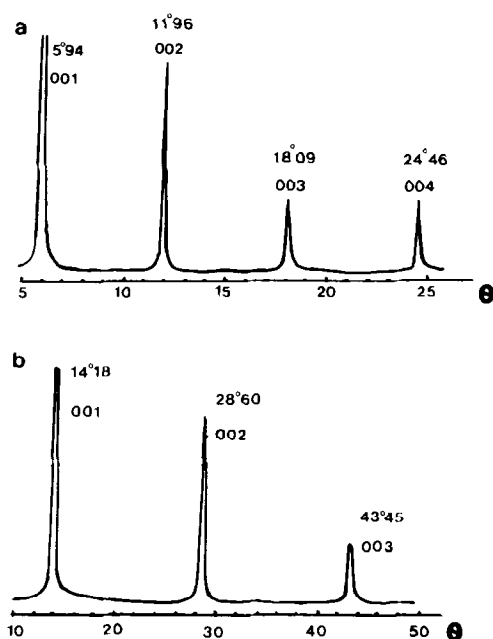


FIG. 2. Diffraction X-ray spectrum of layer of  $\text{VOPO}_4 \cdot 2\text{H}_2\text{O}$  (a) deposited onto a platinum grid and of  $\text{VOPO}_4 \cdot \text{H}_2\text{O}$  (b) ( $150^\circ\text{C}$  or under vacuum).

The anisotropy of the layer is conserved during a thermal dehydration of the compound. An X-ray analysis performed on a high-temperature device shows that around  $100^\circ\text{C}$ , a new basal spacing  $d = 6.30 \text{ \AA}$  is observed, corresponding to  $\text{VOPO}_4 \cdot \text{H}_2\text{O}$  while beyond  $200^\circ\text{C}$  the basal spacing decreases down to  $d = 4.11 \text{ \AA}$  corresponding to  $\text{VOPO}_4$ . A spontaneous rehydration is observed when the sample is kept at room temperature again. It is however very fast and directly leads to  $\text{VOPO}_4 \cdot 2\text{H}_2\text{O}$  ( $d = 7.41 \text{ \AA}$ ). The monohydrate  $\text{VOPO}_4 \cdot \text{H}_2\text{O}$  cannot be observed in such conditions. It can, however, be obtained at room temperature, under vacuum ( $P = 10^{-2} \text{ mm Hg}$ ) where a basal spacing  $d = 6.24 \text{ \AA}$  is observed (Fig. 2b).

It has to be pointed out that more hydration steps can also be obtained at room temperature. Therefore a colloidal solution is

deposited onto a glass substrate and studied by X-ray diffraction, in reflection geometry, before the layer is completely dry. The observed pattern is illustrated in Fig. 3a. It is typical of a regular stacking along the  $c$  axis, perpendicular to the substrate, but the basal spacing,  $d = 10.2 \text{ \AA}$ , is larger than the one corresponding to  $\text{VOPO}_4 \cdot 2\text{H}_2\text{O}$  ( $d = 7.41 \text{ \AA}$ ). The increase  $\Delta d = 2.8 \text{ \AA}$  of the basal spacing corresponds to the Van der Waals diameter of a water molecule, suggesting the intercalation of one more water layer. This hydrated phase is not stable under ambient conditions. The X-ray pattern typical of  $\text{VOPO}_4 \cdot 2\text{H}_2\text{O}$  is again observed after about half an hour (Fig. 3c). During an intermediate period of time the two 00/ diffraction patterns corresponding to  $d = 10.2$  and  $d = 7.41 \text{ \AA}$  are observed (Fig. 3b).

Figure 4a shows TEM micrographs (JEOL 100 CX II Centre de Spectrochimie Paris VI) of colloidal particles of  $\text{VOPO}_4 \cdot \text{H}_2\text{O}$  ( $d = 6.24 \text{ \AA}$ ). The dehydration ( $\text{VOPO}_4 \cdot 2\text{H}_2\text{O} \rightarrow \text{VOPO}_4 \cdot \text{H}_2\text{O}$ ) occurs without altering the lamellar morphology of the crystallites. The platelet crystals (Fig. 4b) of the hydrate have well defined out lines and present always the same plane indexed as (010) (Fig. 4c). All diffraction diagrams are similar showing that the particles are oriented in the same way. On a ultra high resolution diagram (Fig. 4d) it is possible to see parallel rows which form the layers.

### Electron Spin Resonance Study

$\text{VOPO}_4$  always contains some V(IV) ions that are thought to be responsible for its catalytic properties (1). An ESR study of those V(IV) ions ( $S = \frac{1}{2}$ ,  $I = \frac{7}{2}$ ) was then performed on a thick layer deposited onto a plexiglass rod having a plane face about  $5 \times 10 \text{ mm}$ . These ESR spectra are shown in Fig. 5 for different orientations of the layer in the magnetic field.

Two remarks can be made: (1) These

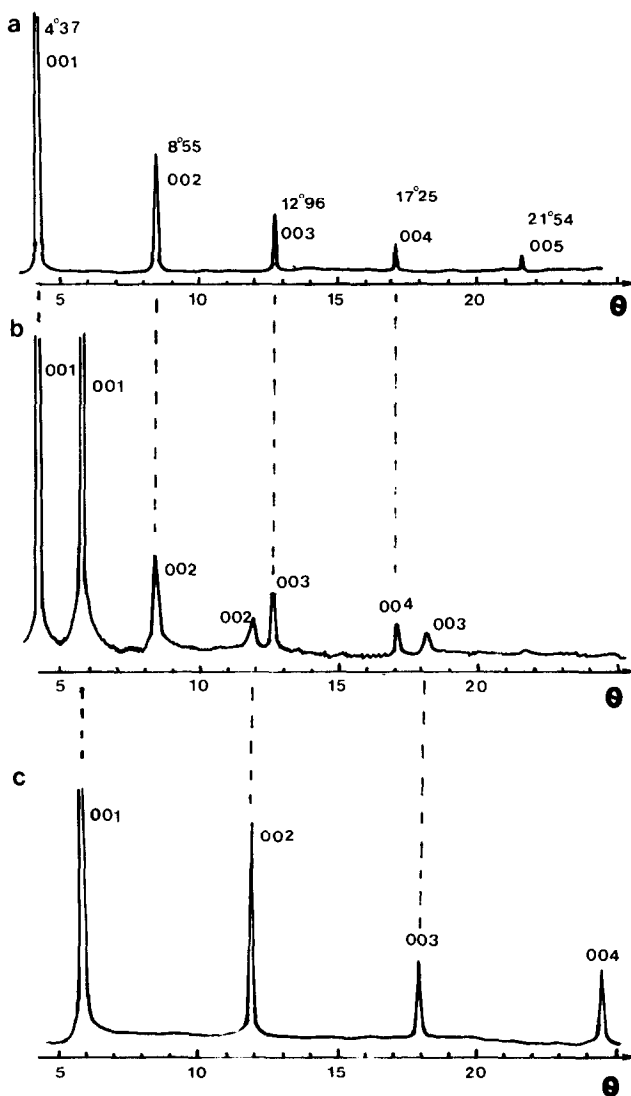


FIG. 3. Diffraction X-ray spectra of (a)  $\text{VOPO}_4 \cdot 3\text{H}_2\text{O}$ ; (b)  $\text{VOPO}_4 \cdot 3\text{H}_2\text{O} + \text{VOPO}_4 \cdot 2\text{H}_2\text{O}$ ; (c)  $\text{VOPO}_4 \cdot 2\text{H}_2\text{O}$ .

spectra do not look like usual powder spectra at all. Their lineshape is quite similar to what would be observed with a single crystal. (2) The position of the eight hyperfine lines strongly depends on the magnetic field orientation, as for a single crystal.

These observations suggest some orientation of the colloidal particles arising from their strong anisotropy. This is the first time

that such an anisotropic spectrum is shown for  $\text{VOPO}_4 \cdot 2\text{H}_2\text{O}$ . On the contrary, previous spectra, already published in the literature, were made with nonoriented particles and therefore looked like usual powder spectra (12).

The orientation dependence of the ESR spectrum shows that the paramagnetic ions  $\text{V(IV)}$  lie in an axial crystal field. They can



FIG. 4. TEM micrographs of particles of colloidal  $\text{VOPO}_4 \cdot \text{H}_2\text{O}$ : (a) general view; (b) crystallite corresponding to diffraction (c); (c) diffraction diagram; (d) UHR diagram.

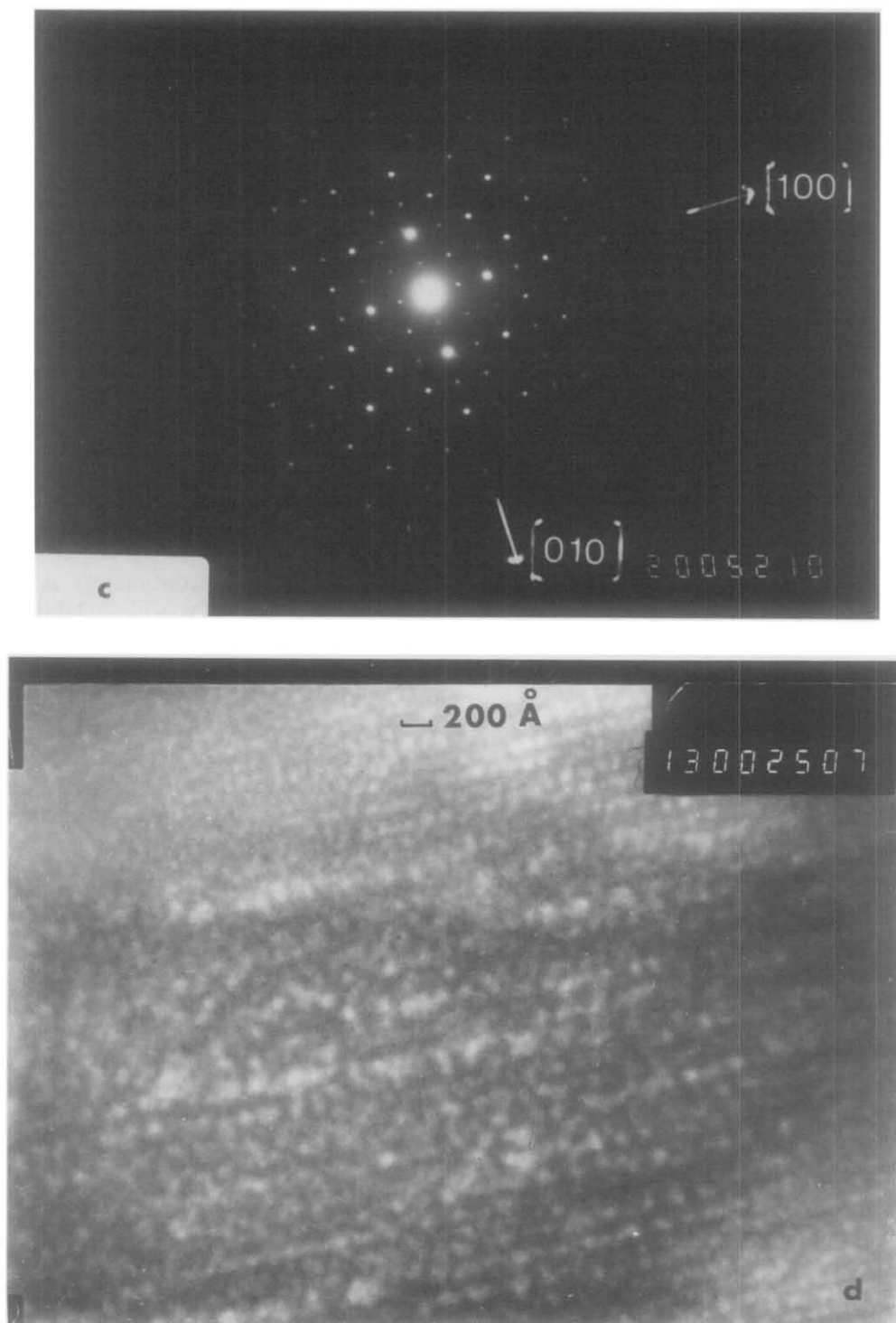


FIG. 4—Continued.

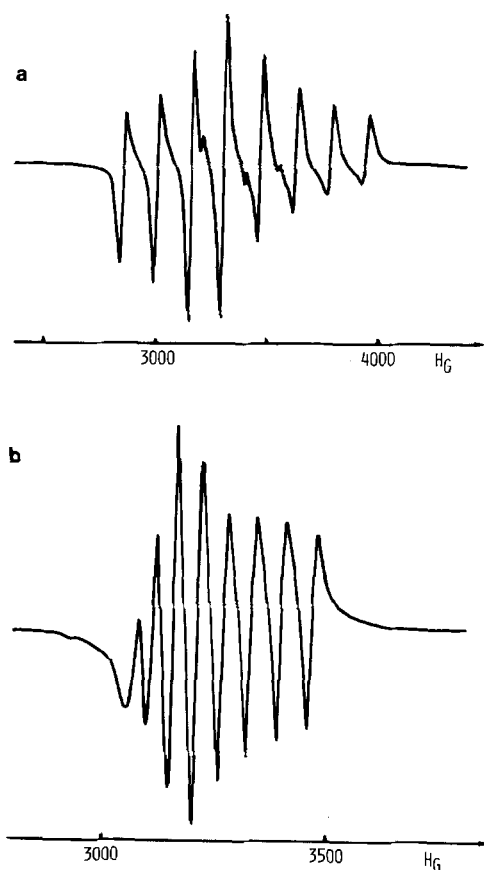


FIG. 5. ESR spectra of a  $\text{VOPO}_4 \cdot 2\text{H}_2\text{O}$  layer: (a) magnetic field perpendicular to the substrate; (b) magnetic field parallel to the substrate.

be described by the usual spin Hamiltonian:

$$\mathcal{H} = g_{\parallel}\beta H_z S_z + g_{\perp}\beta(S_x H_x + S_y H_y) + A_{\parallel}S_z I_z + A_{\perp}(S_x I_x + S_y I_y)$$

where the main axis  $z$  of  $g$  and  $A$  tensors is parallel to the  $c$  axis of the colloidal particles and therefore perpendicular to the substrate. Because of the strong anisotropy of the ESR spectrum, accurate measurements of the position of the hyperfine lines can be performed along both parallel and perpendicular positions, leading to

$$\begin{aligned} g_{\parallel} &= 1.938 & A_{\parallel} &= 192 \text{ G.} \\ g_{\perp} &= 1.982 & A_{\perp} &= 69 \text{ G.} \end{aligned}$$

Such parameters are quite close to those measured for  $\text{V}_2\text{O}_5$  single crystals (13) suggesting that the oxygen polyhedra around vanadium ions is almost the same in both cases, i.e., a square pyramid  $\text{VO}_5$  with a short  $\text{V}=\text{O}$  double bond along the  $c$  axis. It has to be pointed out however that the ESR parameters are actually closer to those observed on  $\text{V}_2\text{O}_5 \cdot n\text{H}_2\text{O}$  gels (14) or the hydrated vanadyl ion  $\text{VO}(\text{H}_2\text{O})_5^{2+}$  (15). This suggests that  $\text{V}(\text{IV})$  ions in  $\text{VOPO}_4 \cdot 2\text{H}_2\text{O}$  are at least partially solvated, one water molecule being presumably bonded along the  $z$  axis, opposite to the  $\text{V}=\text{O}$  bond.

#### Infrared Study of the Water in Hydrated $\text{VOPO}_4$

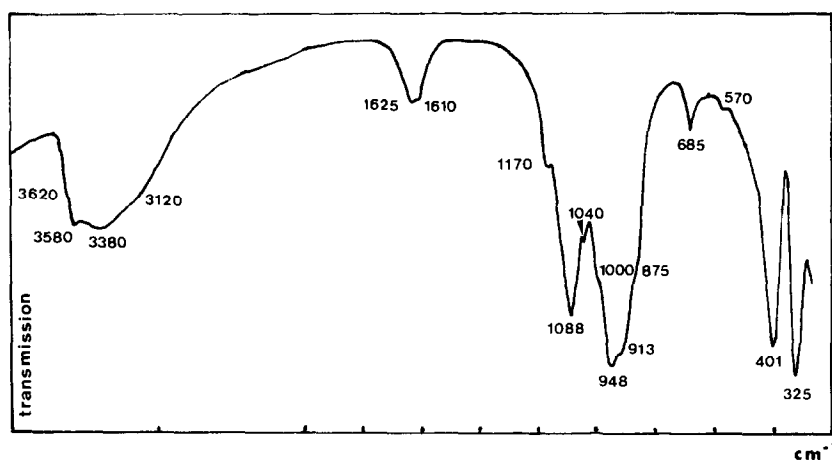
Infrared spectra were recorded on a Perkin Elmer 580 spectrometer. A thin  $\text{VOPO}_4 \cdot 2\text{H}_2\text{O}$  deposit was obtained from a diluted colloidal "solution" (0.1–0.5 mole/liter) onto a fluorine disk ( $\phi$  35 mm  $\times$  2 mm). The IR spectrometer was equipped with a special device to study the sample under vacuum or under some  $\text{H}_2\text{O}$  or  $\text{D}_2\text{O}$  vapor pressure. Dichroic experiments were made by rotating the sample (16),  $\alpha$  being the angle between the IR beam and the perpendicular to the disk. IR spectra were also recorded with KBr pellets.

#### IR Spectrum between 4000 and 300 $\text{cm}^{-1}$

The infrared absorption spectrum of  $\text{VOPO}_4 \cdot 2\text{H}_2\text{O}$  is shown in Fig. 6; band positions are reported in Table I. Water molecules stretching and bending modes can be seen around 3500 and 1600  $\text{cm}^{-1}$ . They will be studied in more detail later.

Between 600 and 1200  $\text{cm}^{-1}$  we have the absorption bands corresponding to  $\text{P}-\text{O}$  and  $\text{V}-\text{O}$  stretching, while below 600  $\text{cm}^{-1}$   $\text{O}-\text{V}-\text{O}$  and  $\text{O}-\text{P}-\text{O}$  bending modes appear (Table I).

All these frequencies are typical of  $\text{VOPO}_4 \cdot 2\text{H}_2\text{O}$  (17). Their analysis has already been published in the case of  $\text{VOPO}_4$

FIG. 6. IR spectrum of colloidal VOPO<sub>4</sub> · 2H<sub>2</sub>O in KBr pellet.

(18). We have therefore restricted our study to the hydration process of VOPO<sub>4</sub> and to the position of water molecules in colloidal VOPO<sub>4</sub> · nH<sub>2</sub>O.

#### Hydration of VOPO<sub>4</sub>

Figure 7 shows the evolution of the IR spectrum of colloidal VOPO<sub>4</sub> as a function of the water vapor pressure.

TABLE I  
ABSORPTION INFRARED BANDS OF VOPO<sub>4</sub> · 2H<sub>2</sub>O

VOPO <sub>4</sub> 2H <sub>2</sub> O (2)	Colloidal VOPO <sub>4</sub> 2H <sub>2</sub> O (Our work)	Attribution (2)
3540 F	3620	ν(OH)
3520 ep	3580	
3350 ep	3380	
3180 ep	3120	
1620 f	1625	δ(HOH)
1590	1610	
1160 ep	1170 f	ν <sub>as</sub> (P—O)
1072 F	1088 F	
1022 ep	1040 f	ν(V=O)
980 ep	1000	
940 TF	948 F	ν V—OH
900 ep	913 ep	ν P—O
860 ep	875 ep	δ(V—OH) or (P—OH)
672 f	685 f	
560 ep	570 f	δ <sub>as</sub> O—P—O
420 ep		δ <sub>s</sub> O—P—O
395 F	401 F	
320 F	325 F	

Under vacuum (Fig. 7a) ( $P \cong 2.10^{-2}$  mm Hg), very sharp IR bands are seen around 3630, 3540, and 1626 cm<sup>-1</sup>. The sharpness of these bands suggest that all water molecules vibrate in the same way as is observed for single crystals hydrates (19, 20). Bands at 3540 and 1626 cm<sup>-1</sup> are strongly dichroic. The corresponding transition moment must then be parallel to the IR beam indicating that the C<sub>2</sub> axis of the water molecule should be perpendicular to the substrate (Fig. 8). According to X-ray diffraction, this sample corresponds to a basal spacing  $d = 6.24 \text{ \AA}$  i.e., VOPO<sub>4</sub> · H<sub>2</sub>O.

New bands appear at 3350 and 1608 cm<sup>-1</sup> for  $P/P_0 \cong 0.5$  above the sample (Fig. 7c). Their width is somewhat larger and they are not dichroic. Two other bands are observed at 3603 and 3518 cm<sup>-1</sup>. Only the first one remains dichroic. According to X-ray diffraction, the sample correspond to VOPO<sub>4</sub> · 2H<sub>2</sub>O, in which two different kinds of water molecules seem to coexist.

#### Deuteration of VOPO<sub>4</sub> · H<sub>2</sub>O

Figure 9 gives the IR spectrum of a VOPO<sub>4</sub> · H<sub>2</sub>O sample, kept under vacuum, during a progressive deuteration.

All spectra suggest the occurrence of a



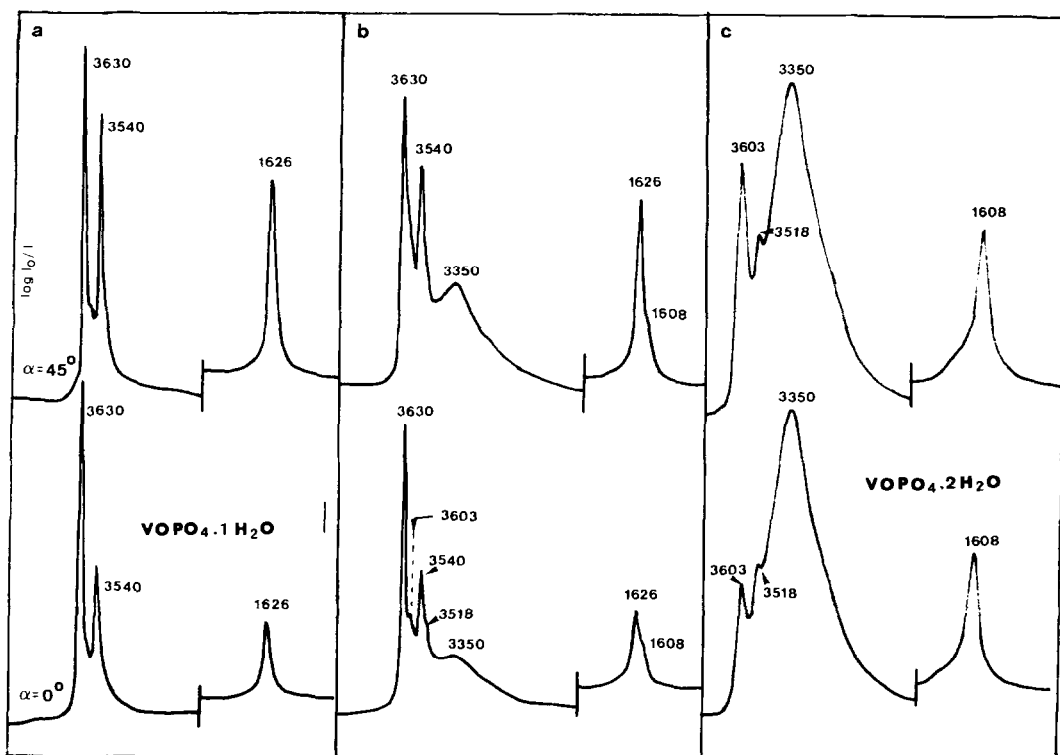


FIG. 7. Stretching and bending bands of water molecules: (a) under vacuum  $P = 10^{-2}$  mm Hg; (b) intermediate pressure; (c) with pressure  $P/P_0 \cong 0.5$ .

single well-defined kind of water molecule. This appears quite obviously when enough deuterium has been introduced so that only isolated  $H_2O$  molecules remain diluted among  $D_2O$  and  $HOD$  species. A single decoupled bending band at  $1618\text{ cm}^{-1}$  is observed for  $H_2O$  molecules. Similarly only one bending mode appears at  $1198\text{ cm}^{-1}$  when the first  $D_2O$  molecules are formed during the deuteration process.

Two new bands appear at  $1432$  and  $1420\text{ cm}^{-1}$  corresponding to the bending of  $HOD$  species, suggesting that water molecules have the  $C_s$  symmetry with two nonequivalent  $OH$  bonds. One of the bonds should be involved in a stronger hydrogen bond than the other one. The  $HOD$  species for one of the bands involves the  $O-D$  bond with the stronger hydrogen bond while the other in-

volves the  $O-H$  bond with the stronger hydrogen bond.

Two  $OD$  stretching bands at  $2610$  and  $2665\text{ cm}^{-1}$  develop at the first step of the

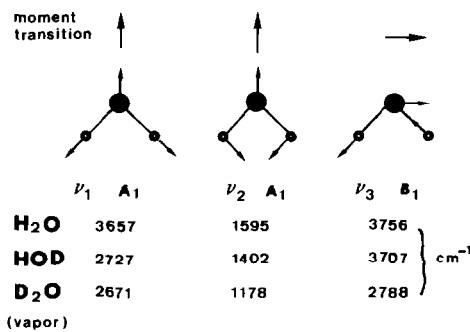


FIG. 8. Transition moment of the IR movements of the water molecule.

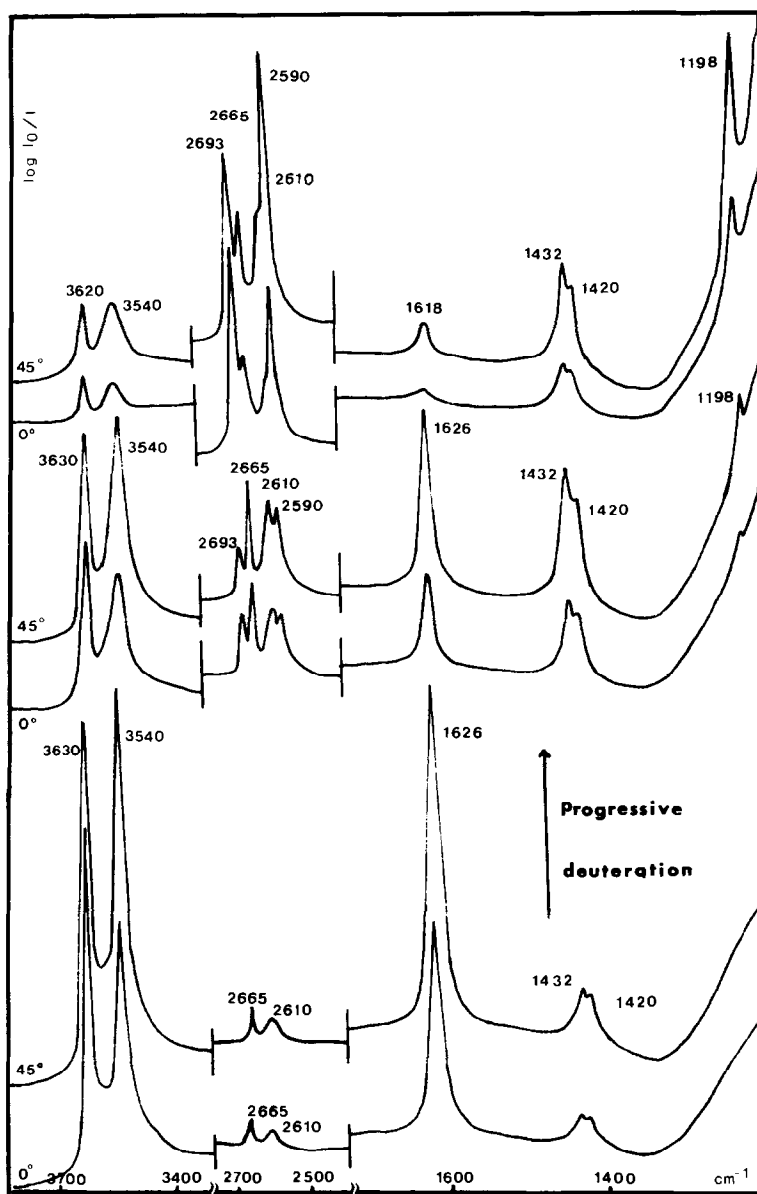


FIG. 9. IR spectra of VOPO<sub>4</sub> · H<sub>2</sub>O during a progressive deuteration.

deuteration process when no D<sub>2</sub>O bending band appears. This means that there are only two kinds of OD groups; when the ratio of deuterium atoms increases, four OD stretching bands develop (Fig. 10). Two of them, at 2665 and 2610 cm<sup>-1</sup>, appear as

soon as D<sub>2</sub>O is introduced. They correspond to OD stretching of HOD species. Their position does not move any further suggesting a strongly decoupled system arising from very different hydrogen bonds (21, 22). Two other bands at 2693 and 2590

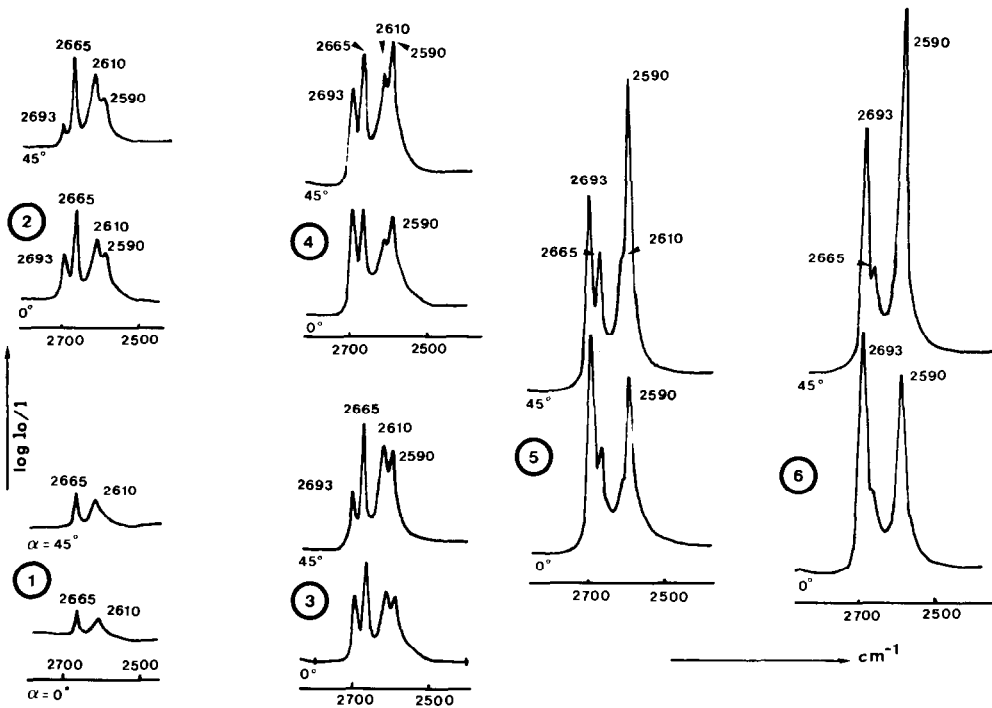


FIG. 10. OD stretching bands upon a progressive deuteration for a  $\text{VOPO}_4 \cdot \text{H}_2\text{O}$  sample, the progressive deuteration is coming from 1 to 6.

$\text{cm}^{-1}$  grow in intensity upon deuteration. They correspond to coupled stretching OD vibrations of  $\text{D}_2\text{O}$  molecules. A correlation can be established between the decoupled OH and OD stretching frequencies and the hydrogen bond length (19, 23, 24). In our case it would correspond to  $\text{O} \cdots \text{O}$  distances of 2.8 Å in one case and more than 3.1 Å in the other.

A strongly dichroic behaviour is observed on the bending band at  $1626 \text{ cm}^{-1}$ . Its intensity is much smaller for  $\alpha = 0$ , the  $I_{45^\circ}/I_{0^\circ}$  ratio being of about 1.62. Such a dichroism is also observed on the other bending bands and with the symmetrical stretching band  $\nu_s$  ( $3540 \text{ cm}^{-1}$ ). This suggests that the transition moments of the corresponding motions should be parallel to the IR beam. The  $C_2$  symmetry axis of the water molecules is then perpendicular to the substrate.

A slight dichroism can be also observed on the lower frequency ( $2610 \text{ cm}^{-1}$ ) stretching band corresponding to OD groups involved in a stronger hydrogen bond. It is thus likely that the orientations of both OH are not absolutely symmetric. The OH group involved in the hydrogen bond should be closer to the perpendicular direction than the other one (Fig. 11).

Such observations were made previously with natrolite (21, 22).

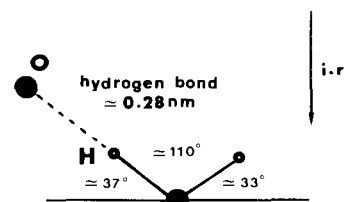


FIG. 11. Position model of the water molecule in colloidal  $\text{VOPO}_4 \cdot \text{H}_2\text{O}$ .

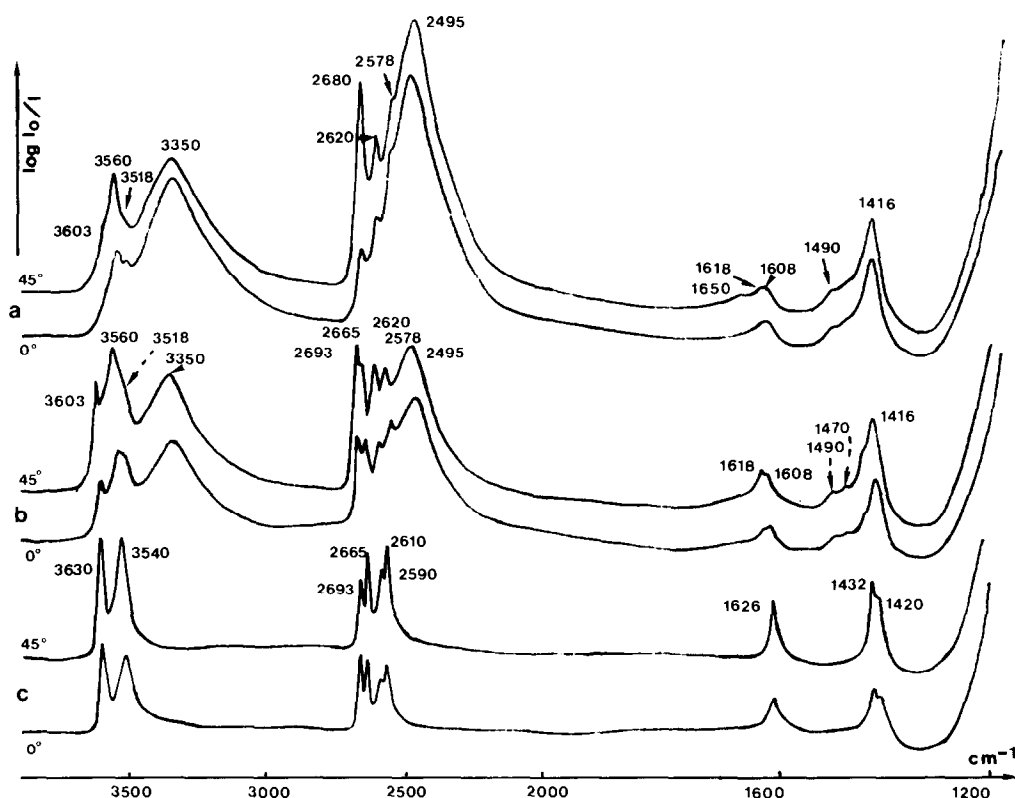


FIG. 12. IR spectra of VOPO<sub>4</sub> · nH<sub>2</sub>O upon partial deuteration: (a) VOPO<sub>4</sub> · H<sub>2</sub>O ( $P = 10^{-2}$  mm Hg); (b) intermediate pressure; (c) VOPO<sub>4</sub> · 2H<sub>2</sub>O ( $P/P_0 \cong 0.5$ ).

### Colloidal VOPO<sub>4</sub> · 2H<sub>2</sub>O

Hydration of VOPO<sub>4</sub> · 2H<sub>2</sub>O was performed for different water vapor pressures and D<sub>2</sub>O/H<sub>2</sub>O ratio equal to one. The corresponding IR spectra are shown in Fig. 12. They suggest the presence of at least two different kinds of H<sub>2</sub>O:

The first one corresponds to strongly hydrogen-bonded water molecules. The IR bands are not dichroic. Their position at 3350, 1608, and 2495, 1416, 1185 cm<sup>-1</sup> is close to what is observed in ice. Their intensity increases when the water pressure above the sample increases.

The second one corresponds to less strongly hydrogen-bonded water mole-

cules. Their relative intensity decreases and their position is slightly shifted when the water pressure increases. The higher frequency band at 3603 cm<sup>-1</sup> appears to be dichroic. It corresponds to OH groups almost perpendicular to the substrate.

### V=OH and P=OH Bands

We have been discussing only OH bonds belonging to water molecules. V—OH and P—OH bonds could also be detected in our samples. Their corresponding bands occur around 950 and 680 cm<sup>-1</sup>. However, no modification has been observed on the spectra upon deuteration. We therefore do not have enough experimental data to discuss this point.

## Discussion and Conclusion

The crystallographic structure of  $\text{VOPO}_4 \cdot 2\text{H}_2\text{O}$  is now well known (4–8). It is a layered structure, made of  $(\text{VOPO}_4)_n$  sheets where  $(\text{VO}_5)$  chains are linked together by  $(\text{PO}_4)$  tetrahedra (Fig. 1). Much less however is known about the position of water molecules (9). The strong anisotropy of the layers deposited from  $\text{VOPO}_4 \cdot 2\text{H}_2\text{O}$  colloidal solutions gives us some more information.

Under vacuum, the monohydrate  $\text{VOPO}_4 \cdot \text{H}_2\text{O}$  is obtained. The IR spectra shows that a single very well defined  $\text{H}_2\text{O}$  species is observed. Its main axis is nearly perpendicular to the substrate, i.e., parallel to the  $c$  axis of the  $\text{VOPO}_4$  lattice according to X-ray diffraction data. These  $\text{H}_2\text{O}$  molecules with  $C_s$  symmetry, are not hydrogen bonded together but one of the OH bond is involved in an hydrogen bond of about 0.28 nm that makes an angle of about  $37^\circ$  with the  $\text{VOPO}_4$  layer.

Two positions are possible: the water molecule could be linked to a vanadium ion, along the  $c$  axis opposite to the  $\text{V}=\text{O}$  short bond, or in the cavity limited by two pyramids  $\text{VO}_5$  and two tetrahedra  $\text{PO}_4$ . The question then arises with which oxygen does the hydrogen bond occur? We do not have enough data to give a clear-cut answer, but we may assume that the  $\text{PO}_4^{3-}$  groups should be a more attractive source.

Under a water pressure  $P/P_0 = 0.5$  the  $\text{VOPO}_4 \cdot 2\text{H}_2\text{O}$  phase is obtained in which at least two different kinds of water molecules can be distinguished. Some of them have their  $C_2$  axis along the  $c$  axis while the others have one of their OH bond parallel to the  $c$  axis. These water molecules seem to be hydrogen bonded together near hydrophilic sites and the basal spacing is  $d = 7.41 \text{ \AA}$ . The suggested model is illustrated in Fig. 13.

However, we have to point out that colloidal  $\text{VOPO}_4 \cdot n\text{H}_2\text{O}$  seems to be very sensi-

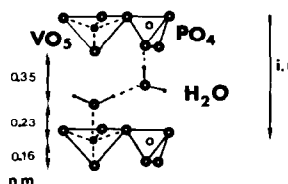


FIG. 13. The water molecules in colloidal  $\text{VOPO}_4 \cdot 2\text{H}_2\text{O}$ .

tive toward water. When the water pressure increases from  $10^{-2}$  to 15 mm Hg, the position of water molecules changes and the first kind of water molecule progressively falls over other position while some supplementary molecules are fastened. We meet three or four kinds of water molecules the position of which at every moment depends on the water pressure. Hydration of  $\text{VOPO}_4$  layers constantly evolves by rocking movements of water molecules near hydrophilic sites.

## References

1. J. W. JOHNSON, A. J. JACOBSON, J. F. BODY, AND S. M. RICH, *Inorg. Chem.* **21**, 3820 (1982).
2. G. LADWIG, *Z. Anorg. Allg. Chem.* **338**, 266 (1965).
3. H. R. TIETZE, *Aust. J. Chem.* **34**, 2035 (1981).
4. E. BORDES AND P. COURTINES, *J. Catal.* **57**, 236 (1979).
5. B. JORDAN AND C. CALVO, *Can. J. Chem.* **51**, 2621 (1973).
6. R. GOPAL AND C. CALVO, *J. Solid State Chem.* **5**, 432 (1972).
7. M. TACHEZ, F. THEOBALD, AND E. BORDES, *J. Solid State Chem.* **40**, 280 (1981).
8. E. BORDES, P. COURTINE, AND G. PANNETIER, *Ann. Chim.* **8**, 105 (1973).
9. M. TACHEZ, F. THEOBALD, J. BERNARD, AND W. HEWAT, *Rev. Chim. Min.* **19**, 291 (1982).
10. E. BORDES AND P. COURTINE, *C.R. Acad. Sci. C*, **274**, 1365 (1972).
11. J. LEMERLE, L. NEJEM, AND L. LEFEBVRE, *J. Inorg. Nucl. Chem.* **42**, 17 (1980).
12. D. BALLUTAUD, E. BORDES, AND P. COURTINE, *Mat. Res. Bull.* **17**, 519 (1982).
13. E. GILLIS AND E. BOESMAN, *Phys. Status Solidi* **14**, 337 (1966).
14. N. GHARBI, C. SANCHEZ, J. LIVAGE, J. LEMERLE,

- L. NEJEM, AND J. LEFEBVRE, *Inorg. Chem.* **21**, 2758 (1982).
15. C. BALLHAUSEN AND H. B. GRAY, *Inorg. Chem.* **1**, 111 (1962).
16. M. T. VANDENBORRE, R. PROST, E. HUARD, AND J. LIVAGE, *Mat. Res. Bull.* **18**, 1133 (1983).
17. E. BORDES, Thèse doc. es Sciences Compiègne, 1979; Doc. de Spec., Paris, 1973.
18. G. T. STRANFORD AND R. A. CONDRADE, *Spectros. Lett.* **17**, 85 (1984).
19. M. FALK AND O. KNOP, (F. Franks, Ed.), Plenum, New York/London, 1973.
20. A. NOVAK, *Structure and Bonding* **18**, 177 (1974).
21. R. PROST, *Spectrochim. Acta A* **30**, 1855 (1974).
22. R. PROST, Thèse doc. es Sciences, Paris, 1975.
23. A. NOVAK, *Inf. R. Spectrosc. Biol. Mol.*, 279 (1979).
24. K. NAKAMOTO, M. MARGOSHES, AND R. E. RUNDLE, *J. Am. Chem. Soc.* **77**, 6480 (1955).